ELSEVIER

Palaeogeography, Palaeoclimatology, Palaeoecology 168 (2001) 311–336

PALAEO

www.elsevier.nl/locate/palaeo

Sr/Ca variations in Cretaceous carbonates: relation to productivity and sea level changes

Heather M. Stoll[a,*], Daniel P. Schrag[b]

[a]*Dept. de Geologia, Universidad de Oviedoc, Arias de Velaso, s/n 33005 Oviedo, Asturias, Spain*
[b]*Dept. of Earth and Planetary Sciences, 20 Oxford St., Harvard University, Cambridge, MA 02168, USA*

Received 28 September 1999; accepted for publication 29 November 2000

Abstract

We present high resolution Sr/Ca measurements on coccolith-dominated pelagic carbonates of Berriasian–Valanginian, Albian–Santonian, and Campanian–Maastrichtian age from DSDP sites and Tethyan land sections. Carbonate Sr/Ca varies by up to 80% over both long and short timescales and may reflect either temporal variations in seawater Sr/Ca or variable Sr partitioning in biogenic carbonates. Numerical models of seawater Sr and Ca budgets indicate that while sea level changes can cause comparably large variations in the seawater Sr/Ca ratio, the timing and pattern of predicted Sr/Ca variations agrees poorly with the carbonate record. Reef crises unrelated to sea level changes may also elevate seawater Sr/Ca, and in some cases, the record of reef crises corresponds to increasing carbonate Sr/Ca. Changes in Sr partitioning, likely due to changes in calcareous nannoplankton productivity, also appear to control carbonate Sr/Ca in these records. Cretaceous carbonate Sr/Ca broadly covaries with indicators of productivity derived from microfossil ecology. Recent studies in sediment core tops and cultures have shown that Sr partitioning in coccolith carbonate is strongly influenced by changes in coccolithophorid growth and calcification rate. Where the effects of changing seawater Sr/Ca can be constrained by independent geological data, carbonate Sr/Ca measurements could provide a valuable perspective on changes in the productivity of calcareous nannoplankton and variations in the carbonate and carbon cycle in the Cretaceous. © 2001 Elsevier Science B.V. All rights reserved.

Keywords: Carbonates; Palaeoclimate; Mesozoic; Geochemical tools

1. Introduction

The Sr/Ca ratio of marine carbonates is controlled both by the Sr/Ca ratio of seawater from which they precipitate, and by environmental and biological effects on the partitioning of Sr in biogenic carbonates. In addition, secondary diagenetic processes can modify the chemistry of ancient carbonates. However, by taking steps to minimize the influence of secondary diagenesis on records of past carbonate chemistry, it is often possible to infer changes in seawater chemistry and/or element partitioning which reflect changes in past environmental and/or oceanographic conditions.

Recent studies in sediment core tops and cultures have shown that Sr partitioning in coccolith carbonate is strongly influenced by changes in coccolithophorid growth and calcification rate (e.g. Stoll and Schrag, 2000b; Stoll et al., 2000; Rosenthal et al., 2000; Stoll et al., in press). Since nannofossil carbonate is the dominant carbonate source in Cretaceous sediments, carbonate Sr/Ca variations may reflect variations in

* Corresponding author.
E-mail address: heather.stoll@asturias.geol.uniovi.es (H.M. Stoll).

0031-0182/01/$ - see front matter © 2001 Elsevier Science B.V. All rights reserved.
PII: S0031 0182(01)00205 X

Table 1
Location and characteristics of sites in this study. References for paleodepth determinations from (a) Thierstein and Roth, 1991; (b) Kuhnt, 1990; (c) Johnson, 1984; (d) Exon et al., 1992

Interval/site	Location	Paleolat.	Paleodepth (m)	Sample res (ky)	Lithology	Comments
Berriasian–Valanginian						
DSDP 534A	Blake–Bahama Basin, N. Atlantic	20 N	2000–4000a	25–50	marly limestone interbedded with nannofossil limestones	
DSDP 603B	N. Atlantic	25 N	4000a	25–50	marly limestone interbedded with nannofossil limestones	
U. Albian–L. Santonian						
Contessa Quarry	Gubbio, Italian Apennines	25 N	1500–2500b	10–20	thick to thin-bedded nanno. limestones	
Santa Ines Section	Caravaca, Spanish Betic Cordillera	25 N	1500–2500b	10–20	thick to thin-bedded and nodular nanno. limestones	complex stratigraphy: minor slumps, folds, and faults
U. Campanian–L. Maast.						
DSDP 516F	Rio Grande Rise, S. Atlantic	30 S	1000–1500c	20–30	nannofossil chalk and clayey nannofossil chalk	
DSDP 762C	Exmouth Plateau, Indian Ocean	45 S	> 500d	20–30	nannofossil chalk and clayey nannofossil chalk	

coccolithophorid productivity. However, seawater Sr/Ca can vary appreciatively over timescales longer than the 1–2 m.y. residence times of Sr and Ca in the ocean. For example, large, rapid increases in seawater Sr/Ca ratios were predicted to accompany large Cretaceous sea level falls that expose Sr-rich shelf sediments to weathering (Stoll and Schrag, 1996). We suggest that the sources of Sr variations in Cretaceous carbonates can be constrained using independent geological data on likely changes in seawater Sr/Ca.

Here we examine variations in the Sr/Ca ratios of deep sea, nannofossil-dominated carbonates from three time intervals in the Cretaceous period: the Berriasian–Valanginian, Late Albian–Early Santonian, and Late Campanian to Middle Maastrichtian. In the first part of the paper (Section 2), we present precise analyses of Sr/Ca and stable isotopes from over 2100 samples, with multiple sites for each time interval. This data set is distinguished from previous published Cretaceous minor element records (e.g. Renard, 1986) by its much higher resolution and tight age correlation among multiple sites.

In the second part of the paper (Section 3), we use numerical models of seawater Sr and Ca budgets to evaluate which variations in carbonate Sr/Ca ratios could be accomplished by changes in seawater Sr/Ca. Using sequence stratigraphic and stable isotopic data, we assess the magnitude and timing of likely changes in the Sr/Ca ratio of seawater resulting from weathering of Sr-rich shelf aragonites during sea level falls. Data on ocean crust production rates and Sr isotopic variations in carbonates are used to constrain the effects of past variations in the hydrothermal and riverine Sr and Ca fluxes on seawater Sr/Ca. Potential changes in the fraction of carbonate sedimentation in deep sea vs. shelf settings are compared to the timing of reef crisis and platform drowning events.

Carbonate Sr/Ca variations that cannot be explained by changing seawater Sr/Ca ratios are likely to reflect changes in Sr partitioning in biogenic carbonates. In the third section of the paper (Section 4), we discuss how variations in coccolithophorid productivity may influence Sr partitioning in carbonates. To compare geochemical records with other productivity indicators, we compile detailed records of variations in the ecology of planktonic foraminifera and nannofossils that may reflect changes in environmental conditions and productivity. This approach does not lead to an unambiguous interpretation of Cretaceous Sr/Ca variations. However, it suggests some dominant controls over carbonate Sr/Ca ratios during certain intervals. In particular, changes in Sr partitioning, likely related to the productivity of calcareous nannofossils, appear to be an important control on carbonate Sr/Ca in deep sea Cretaceous carbonates. Sr/Ca variations thus provide some insights on variations in the carbon and carbonate cycle during the Cretaceous.

2. Records of Sr/Ca in Cretaceous carbonates

2.1. Sites and analytical methods

We selected sites of deep sea pelagic sedimentation to avoid variations in the mineralogy (aragonite vs. calcite) of the sediments which lead to heterogeneities in Sr partitioning and in diagenetic alteration. The selected sites are predominantly carbonate-rich and the carbonate fraction is comprised almost entirely by calcareous nannofossils (Arthur and Fisher, 1977; Exon et al., 1992). The location, paleolatitude and paleodepth, and lithology of the selected sites is given in Table 1 along with the sampling resolution of this study.

For both Sr/Ca and minor element determinations, bulk carbonate was analyzed. Bulk carbonate analysis is ideal for the high resolution required by this study because it facilitates rapid analysis of a large number of samples and requires very little core material. Using bulk carbonate rather than specific fractions of the sediment may introduce additional sources of variability in the record, both from changes in the components of the sediments and from more advanced alteration in some components. Changes in the components of sediments are minimal since calcareous nannofossils dominate carbonate in all sediments. In addition, comparisons of stable isotopic values of bulk carbonate and microfossil separates shows that bulk carbonate accurately records isotopic changes over Late Quaternary glacial cycles (Shackleton et al., 1993; Schrag et al., 1995).

Berriasian–Valanginian and Campanian–Maastrichtian age samples were crushed, weighed, dissolved in 1 N acetic acid, and centrifuged to separate the insoluble residue. Sr concentrations of the dissolved carbonate

fraction were determined by flame Atomic Absorption Spectrometry on a Perkin Elmer model 3100 instrument at Princeton University, with the addition of 2% LaCl as a spectral releasing agent. Ca concentrations were determined from the fraction of insoluble residue, calculated as $CaCO_3$. Precision, as determined by analysis of replicate pairs, is better than 2% (1 SD). Evaluation of cleaning procedures showed that ion exchange cleaning steps had a negligible effect on the variations in these samples.

Late Albian to Santonian samples from Spain and Italy were drilled from land exposures. To minimize interferences from cations adsorbed on noncarbonate components, the precleaning procedure of Apitz (1991) was utilized. Approximately 100 mg of sample powder was added to a centrifuge tube. The sample was then shaken with 50 ml of reducing solution (25 g NH_2OH:HCl, 200 ml concentrated NH_4OH, in 300 ml distilled water) for 4–12 h at room temperature. The reducing solution was aspirated off and the sample was then shaken for 10 min with 50 ml of ion exchange solution (1 M NH_4OH), and this solution was aspirated off. Finally, the sample was dissolved in 12 ml of 0.1 M ammonium acetate-acetic acid buffer. Sr/Ca ratios for these samples were determined using Inductively Coupled Plasma Emission Spectroscopy on a Jobin-Yvon simultaneous 46-P instrument at Harvard University with repeated analysis of a reference standard after every 20 samples for drift correction. Precision averages were 5% for Sr/Ca ratios (1 SD) from the Italian section, due to interference of La added during sample preparation in anticipation of analysis via Atomic Adsorption. Precision averages were 2% for Sr/Ca ratios from the Spanish section, prepared without addition of La.

Stable isotopic data for all samples were collected on a gas source mass spectrometer at Princeton University and Harvard University. Approximately 2 mg of bulk sediment was loaded into a stainless steel capsule and placed in a drying oven for 48 h at 50°C. Samples were dissolved on line in a common acid bath of orthophosphoric acid at 90°C. Precision (1 s) averages were 0.07‰ for oxygen and 0.05‰ for carbon.

2.2. Diagenetic alteration of Sr/Ca in carbonates

Quantitative studies on the fate of Sr in carbonate during diagenesis permit us to assess the likely influence of diagenesis on our Sr/Ca records (e.g. Richter and DePaolo, 1987, 1988; Richter and Liang, 1993; Richter, 1996). The Sr content of primary biogenic calcites is much higher than secondary equilibrium abiogenic calcites, so diagenetic recrystallization results in loss of Sr to porewaters. As sediments are buried deeper than ~200 m, Sr loss is limited by the slow rate of diffusion relative to burial and an equilibrium is established between pore water Sr concentrations and the Sr concentration of recrystallizing carbonate. Consequently, Sr loss from sediments occurs only during early burial stages and is typically limited to 15–25% of the original Sr concentration at the moderate to high sedimentation rates characteristic of these Cretaceous sections (Richter and Liang, 1993). As long as sedimentation is continuous and sediments from the same section have the same recrystallization behavior, they will all lose comparable amounts of Sr. While diagenesis will decrease the mean Sr/Ca ratio of the sediments, primary variations will be preserved, although partially attenuated. For this study, we focus on variations in Sr/Ca ratios in sediments and not on absolute values of Sr/Ca ratios.

Differential alteration of sediments within the section may result in a potentially more problematic consequence of diagenesis, the creation of high-frequency Sr/Ca variations where none existed in the primary sediment. Such differential alteration would require variation in the character or reactivity of the sediments, so that some sediments recrystallize more rapidly, and hence to a greater extent, than adjacent sediments. Schlanger and Douglass (1974) suggested that the reactivity, or diagenetic potential,

Fig. 1. Geochemistry of Berriasian–Valanginian sequences vs. sample depth. Crosses indicate all data points and triangles and circles are used to track variations among sediments of limited $CaCO_3$ content as described in the text (circles, $CaCO_3$ from 75 to 85% in 534A, 70–80% in 603B; triangles, $CaCO_3$ from 65 to 75% in 534A, 60–70% in 603B). Significant trends in each panel are highlighted with thin lines: the positive $\delta^{13}C$ excursion starting at the nc2/nc3 boundary in both sites has been noted globally (Lini et al., 1992; Weissert et al., 1998); Sr/Ca begins to increase in both sites slightly before $\delta^{13}C$ increase; small positive $\delta^{18}O$ excursions in the 534A record (just after nc1/nc2 and nc2/nc3 boundaries) cannot be distinguished in the 603B record due to lack of sample coverage at the appropriate intervals. Biostratigraphy from Bralower et al., 1989 and age ties from timescale of Haq et al. (1987).

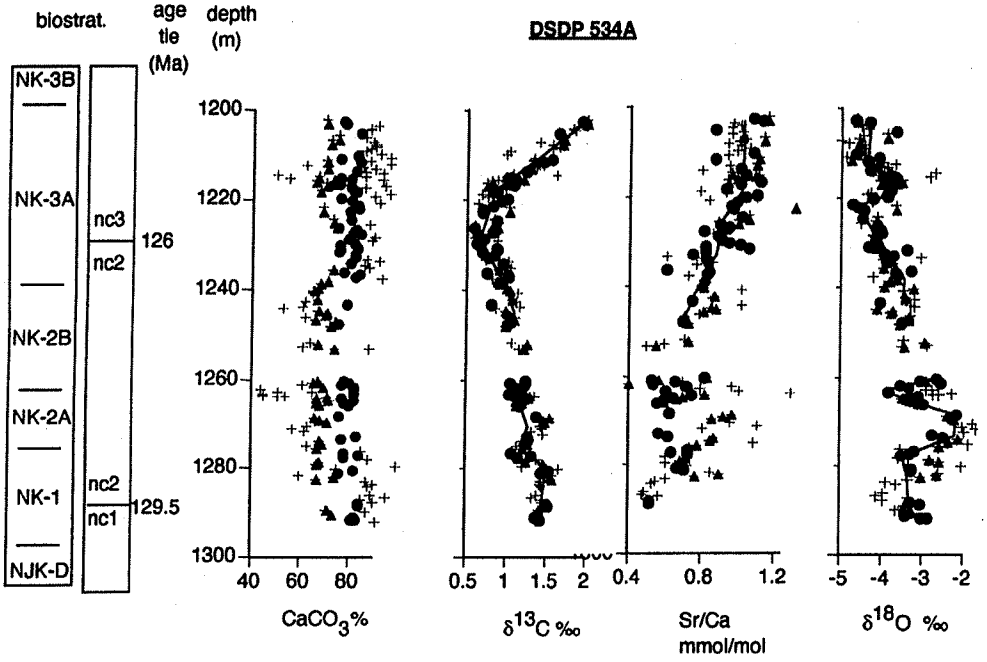
biostrat.
age tie (Ma)
depth (m)
DSDP 534A
NK-3B
NK-3A
NK-2B
NK-2A
NK-1
NJK-D
nc3
nc2
nc2
nc1
126
129.5
1200
1220
1240
1260
1280
1300
40 60 80
CaCO3%
0.5 1 1.5 2
δ13C ‰
0.4 0.8 1.2
Sr/Ca mmol/mol
-5 -4 -3 -2
δ18O ‰

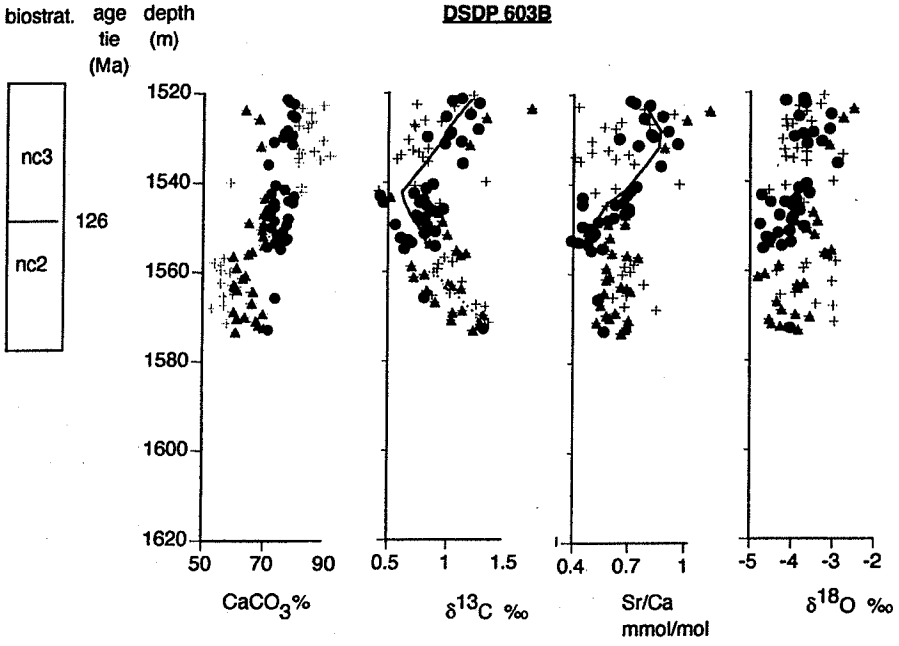
biostrat.
age tie (Ma)
depth (m)
DSDP 603B
nc3
nc2
126
1520
1540
1560
1580
1600
1620
50 70 90
CaCO3%
0.5 1 1.5
δ13C ‰
0.4 0.7 1
Sr/Ca mmol/mol
-5 -4 -3 -2
δ18O ‰

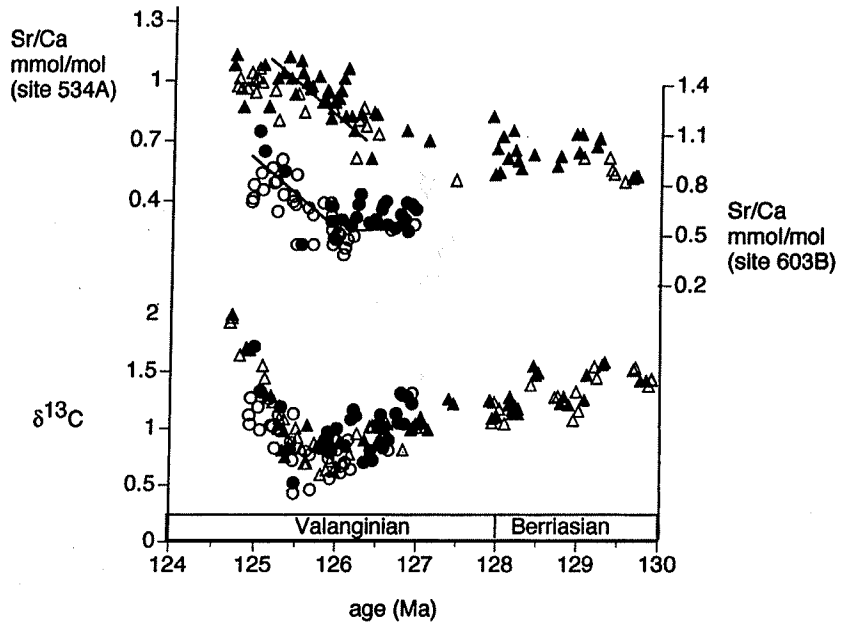

Fig. 2. Correlation of Sr/Ca variations in Berriasian–Valanginian sequences. Correlation via $\delta^{13}C$ as described in Stoll and Schrag (1996). Triangles, from sites 534A, circles from 603B. Filled symbols, $CaCO_3$ 65–75% (60–70% for 603B), open symbols $CaCO_3$ 75–85% (70–80% for 603B). Lines highlight increase in Sr/Ca around 126 Ma.

of carbonate sediments is likely to be controlled by the relative contributions of different nanno- and microfossil assemblages and $CaCO_3$ content. Calculations of recrystallization rate in recent sediments following the method of Richter and Liang (1993) also show that sediments with lower $CaCO_3$ content recrystallize much more slowly than sediments of high $CaCO_3$ (Stoll, unpublished data).

Where sediment lithology is very homogeneous, such as the Contessa and Santa Ines sections, differential diagenesis is not likely to produce large artifacts in Sr/Ca or stable isotopic records (see Stoll and Schrag, 2000a, for a detailed analysis of diagenetic effects on oxygen isotopes in this section). $CaCO_3$ content is relatively constant in these sections and variations in relative abundance of microfossils are not correlated with stable isotopic variations (Stoll and Schrag, 2000a). In other sites where lithology is more variable, time series records of Sr/Ca may contain small artifacts due to more extensive recrystallization and Sr loss in $CaCO_3$-rich sediments. To compare sediments that are likely to have experienced a similar degree of diagenetic alteration, we extracted Sr/Ca time series from a subset of samples with a very narrow range (10%) in $CaCO_3$. In this way, we reduced the probability that trends in Sr/Ca ratios represent artifacts of differential diagenesis.

2.3. Variations in Sr/Ca of Cretaceous carbonates

The geochemical data for all samples are shown in Figs. 1, 3 and 5, together with stable isotopic data, magnetostratigraphy and biostratigraphy used as the

Fig. 3. Geochemistry of Albian–Santonian sequences vs. sample depth. For Contessa Quarry, data points represent 5 point running mean, for Santa Ines data points represent a 3 point running mean. Due to uniform $CaCO_3$ content, time series records include all analyzed samples. The oxygen isotope record is discussed in detail in Stoll and Schrag (2000a). Biostratigraphy for Italian section from Bottacione Gorge (4 km from Contessa Quarry) of Premoli Silva and Sliter (1994). $CaCO_3$ for Bottacione Section from Arthur, 1979. Biostratigraphy of Santa Ines Section from Aguado, 1994.

Contessa Quarry Section, Italy

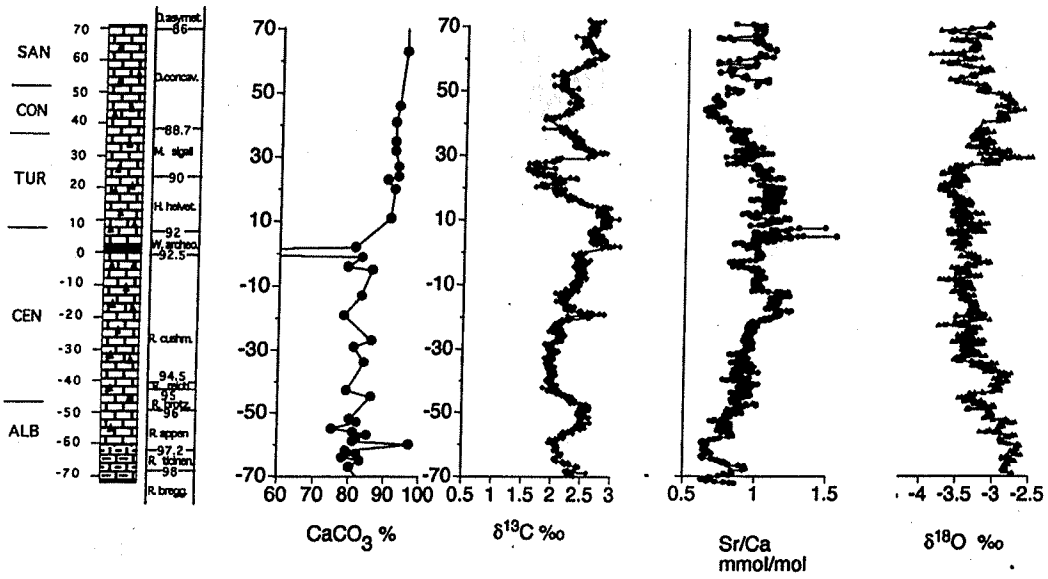

Santa Ines Section, Spain

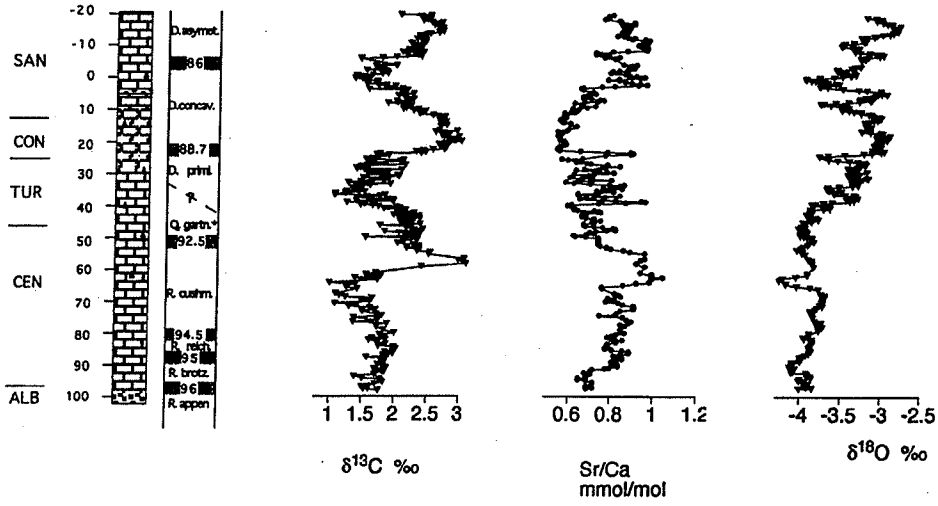

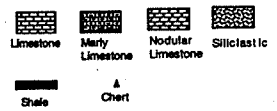

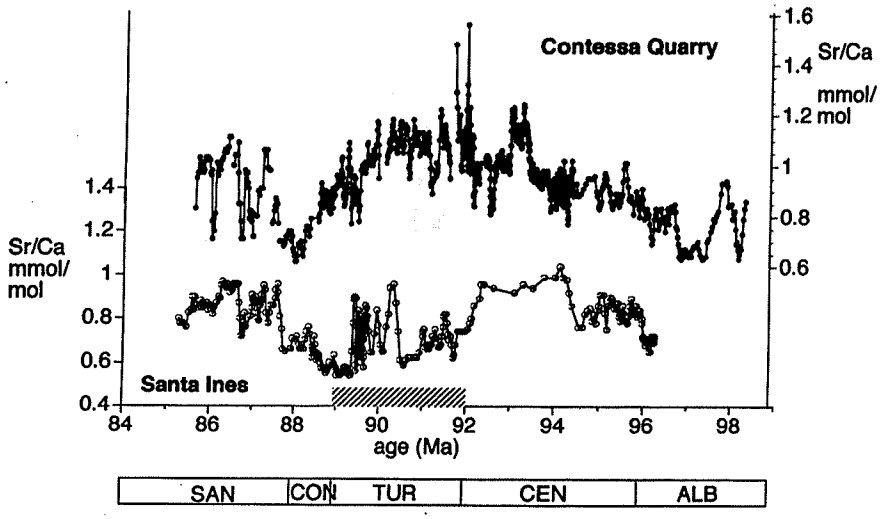

Fig. 4. Comparison of Sr/Ca variations in correlated Albian–Santonian sequences from Contessa Quarry (right axis; data points 5 point running mean) and Santa Ines section (left axis; data points 3 point running mean). Sites were correlated via biostratigraphy and $\delta^{13}C$ variations as described in detail in Stoll and Schrag (2000a). The dashed box marks an interval in the Santa Ines section which could not be characterized biostratigraphically (Aguado, 1994), perhaps due to reworking, influx of shelf sediments, or other stratigraphic complexities.

basis for subsequent correlation of the sections (shown in Figs. 2, 4 and 6). Numerical age assignments for all tie points are based on the timescale of Haq et al. (1987). There is considerable discrepancy in numeric ages for the Lower Cretaceous among the different timescales. We selected the Haq et al. (1987) timescale to facilitate comparison with their sequence stratigraphic sea level curve and not to suggest that it represents the best or most current absolute geochronological data (Figs. 1–6).

The most salient variations in carbonate Sr/Ca are those of the Berriasian–Valanginian interval, when Sr/Ca ratios in both sites ascend gradually by 80% beginning around 126 Ma (Fig. 2). Very gradual trends of Sr/Ca variations over several m.y. also characterize Sr/Ca variations in the Albian–Santonian record from the Contessa Quarry, although smaller brief excursions are superimposed on these trends. Both Contessa and Santa Ines records show Early Cenomanian increases in Sr/Ca, but in Santa Ines, Sr/Ca plateaus and drops sharply after the Cenomanian/Turonian boundary whereas in the Contessa record Sr/Ca remains high until the latest Turonian (Fig. 4). This interval of poor agreement corresponds to the interval which could not be characterized biostratigraphically. In both records, Sr/Ca increases in the Coniacian and Santonian with a synchronous negative excursion around 87 Ma. The Campanian–Maastrictian Sr/Ca records are characterized by multiple rapid (<1 m.y.) oscillations in Sr/Ca, with a larger magnitude positive excursion around 71 Ma (Fig. 6). Some of the more rapid events appear to be reproduced in both sites, and in both sites the highest Sr/Ca ratios occur at 71 Ma.

In the following sections, we investigate whether these variations in carbonate Sr/Ca could be explained by likely variations in seawater Sr/Ca ratios or changes in Sr partitioning in carbonates.

Fig. 5. Geochemistry of Campanian–Maastrichtian sequences vs. sample depth. Crosses indicate all data points and circles are used to track variations among sediments of limited $CaCO_3$ content (80–90% in 762C; 65–75% in 516F) as described in the text. Thin lines highlight pronounced increases in $\delta^{18}O$ in 516F and less pronounced in 762C after the middle of the C33N magnetochron which are consistent with a long term cooling trend observed in foraminiferal $\delta^{18}O$ records (Barrera et al., 1997). Magnetostratigraphy for 762C from Galbrun, 1992, and for 516F from Berggren et al., 1984. Nannofossil events in 762C from Bralower and Siesser, 1992.

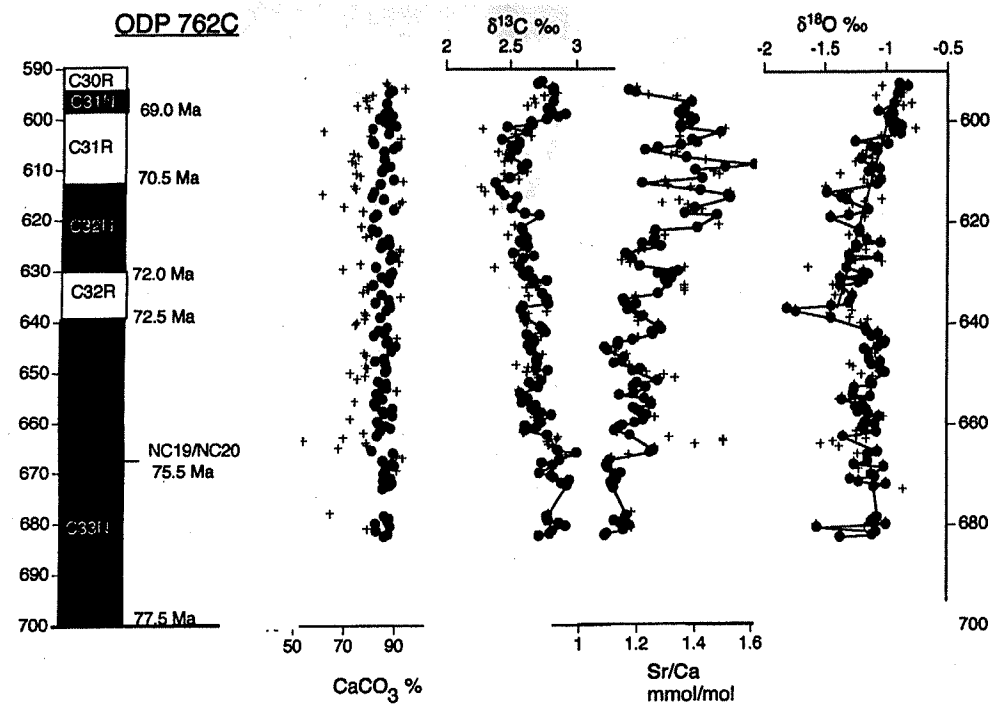
ODP 762C
δ13C ‰
δ18O ‰
C30R
C31R
C32R
69.0 Ma
70.5 Ma
72.0 Ma
72.5 Ma
NC19/NC20
75.5 Ma
77.5 Ma
CaCO3 %
Sr/Ca
mmol/mol

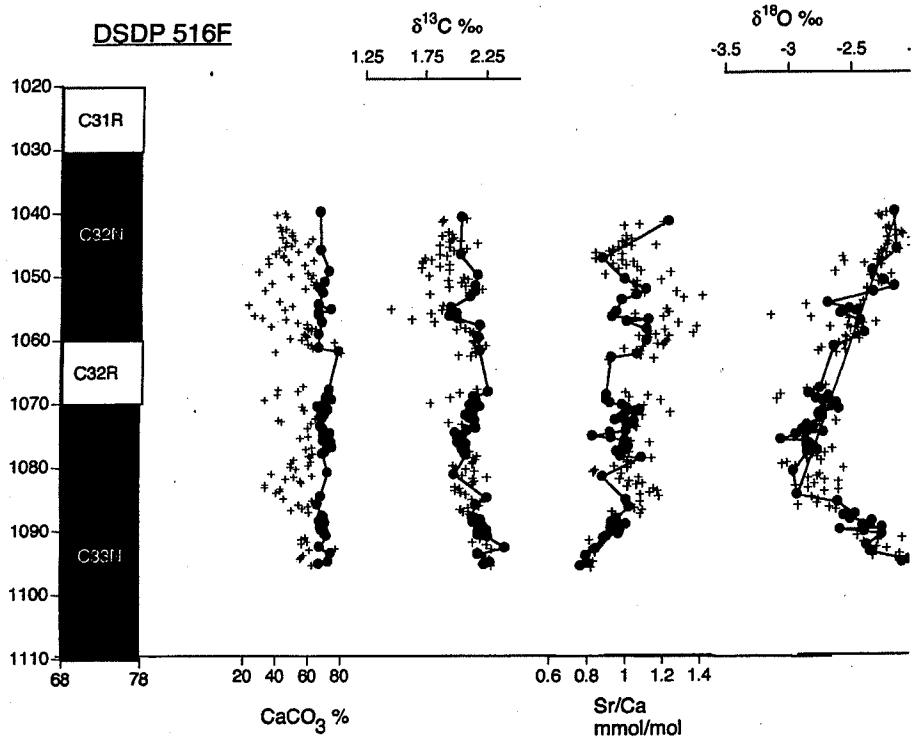
DSDP 516F
δ13C ‰
δ18O ‰
C31R
C32R
CaCO3 %
Sr/Ca
mmol/mol

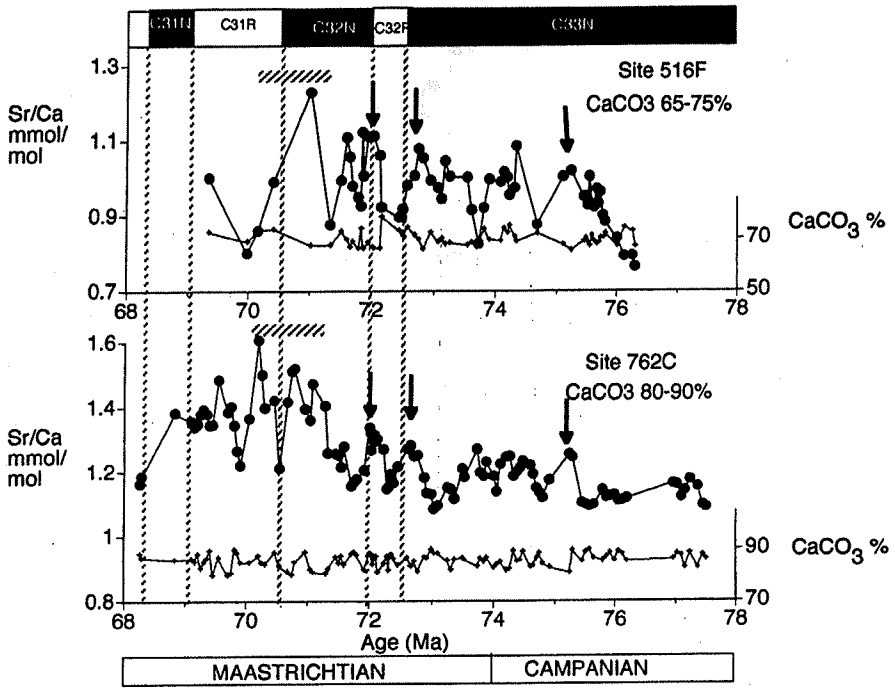

Fig. 6. Comparison of Sr/Ca variations in correlated Campanian–Maastrichtian sequences (filled circles). Samples selected for minimum limited $CaCO_3$ variation as shown in the lowest part of each figure (small diamonds). Magnetostratigraphic basis for correlation is shown at top of figure. For Site 516F, youngest four data points are taken from Renard, 1986. Highest Sr/Ca is noted in both records around 71 Ma (indicated by shaded boxes). Where there is tight magnetostratigraphic control of correlation, small positive excursions may correlate in the two records (indicated by arrows). Thin dashed lines indicate possible correlation of Sr/Ca variations in the C33N interval where magnetostratigraphic control is not tight.

3. Modeling likely variations in seawater Sr/Ca ratios

3.1. Mechanisms for changing seawater Sr/Ca

Sr and Ca are added to the ocean via weathering of continental crust and hydrothermal alteration of mid-ocean ridge basalts, and removed from the ocean in carbonate sediments in shallow shelf and deep ocean settings. The Sr/Ca ratios of hydrothermal fluxes are only about a factor of two larger than those derived from continental weathering. However, modern aragonite-dominated shelf carbonates have Sr/Ca nearly six times higher than calcitic deep sea carbonates. Consequently, the Sr/Ca ratio of seawater is sensitive to the proportion of carbonate removed in aragonitic vs. calcitic sediments (e.g. Graham et al., 1982; Turekian, 1963).

The large fractionation of Sr between shelf and deep sea carbonates has other important consequences for the Sr/Ca ratio of the ocean. When sea level drops, shelf aragonite, exposed to meteoric waters, recrystallizes rapidly to calcite and releases the majority of its Sr while conserving Ca (Schlanger, 1988). This large Sr influx produces a rapid increase in the Sr/Ca ratio of seawater. In the Cretaceous, the Sr/Ca ratio of seawater may have been a more sensitive indicator of rapid sea level changes than today because of higher overall rates of carbonate accumulation and more extensive accumulation of shelf carbonates. Both would increase the impact of shelf weathering on the Sr/Ca ratio of seawater. These combined effects also reduced the residence time of Sr in the Cretaceous ocean, so that rapid changes in Sr fluxes would produce higher amplitude responses in the seawater Sr/Ca ratios. However, the dominance of calcitic

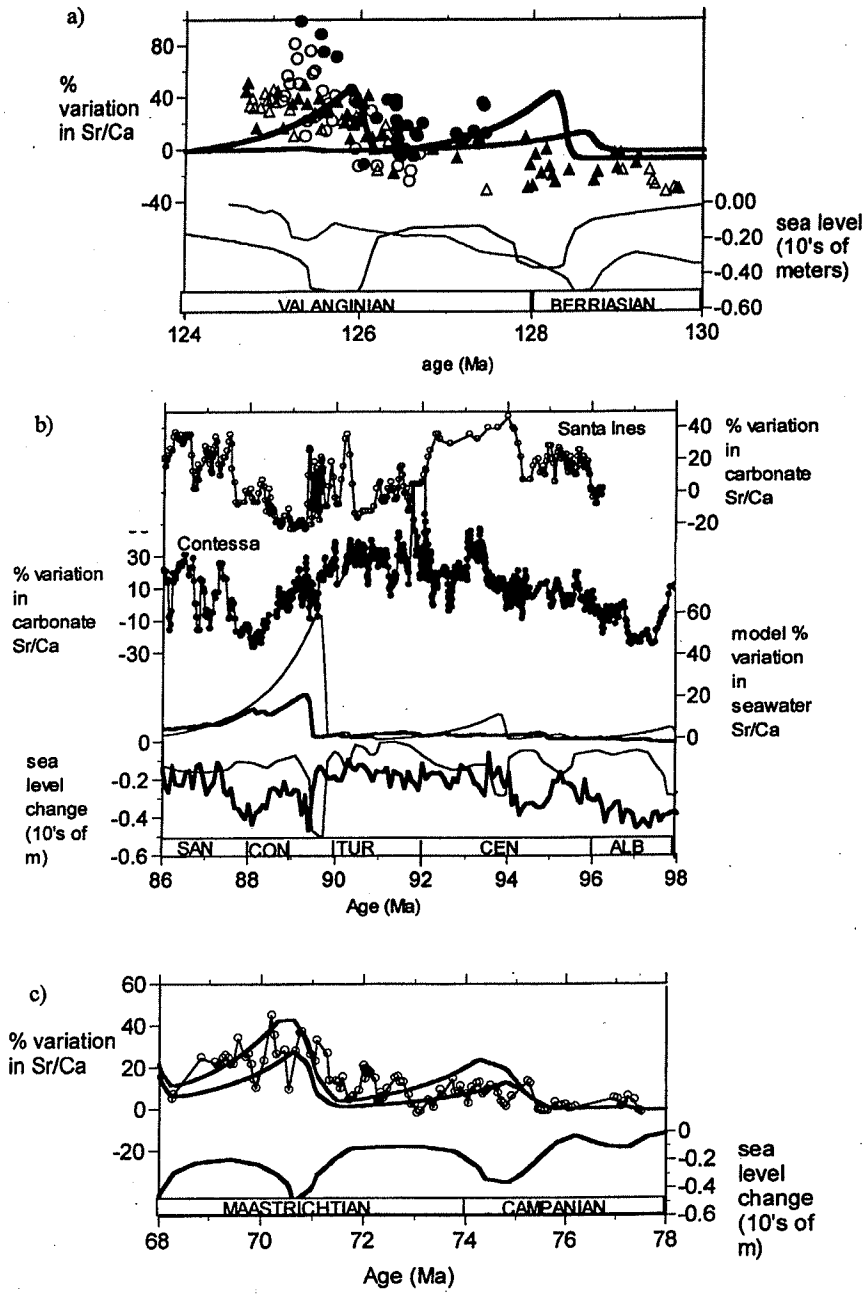

Fig. 7. Likely variations in seawater Sr/Ca resulting from sea level changes, compared with measured carbonate Sr/Ca for Berriasian–Valanginian (a), Albian–Santonian (b) and Campanian–Maastrichtian (c) intervals. Circle and triangle symbols in the upper portion of each figure denote measured carbonate Sr/Ca (samples selected as in Figs. 2, 4 and 6). In (c) a composite Sr/Ca record for 516F and 762C is shown. Modeled variations in seawater Sr/Ca for different sea level histories are shown by bold black and grey lines overlapping (a) and (c) or below (b) the data. The sea level history used for each simulation is shown at the bottom of each figure with a matching line pattern (sea level curves derived from sequence stratigraphic and stable isotope data, as detailed in Appendix B). For all figures, black line indicates model result from sea level forcing of Haq et al. (1987). In (a) and (b) gray line denotes model result from sea level forcing from $\delta^{18}O$ records of DSDP 534A and Contessa Quarry, respectively. In (c) grey line denotes model result from sea level forcing of Haq et al. (1987) including 50% reduction in shelf accumulation during sea level regression. Percent variation in Sr/Ca was calculated as % difference from Sr/Ca ratios at 126.5, 96 and 76 Ma for Berriasian–Valanginian, Albian–Santonian, and Campanian–Maastrichtian, respectively.

rudists in Upper Cretaceous shelf environments may have decreased the amount of Sr available for recrystallization during sea level falls.

Models offer several advantages over merely comparing the timing of sea level changes and reef crises events with Sr/Ca records. Because of the long residence times of Sr and Ca in the ocean, the changes in fluxes accompanying sea level changes and reef crises do not produce instantaneous changes in seawater Sr/Ca. Models illustrate the timing of the ocean's response to these changes. In addition, the models predict the magnitude of changes in seawater Sr/Ca in response to flux changes, subject, of course to uncertainties in estimating model parameters.

3.2. Approach to modeling changes in Cretaceous seawater Sr/Ca

We use a numerical model of the coupled Sr and Ca budgets of the ocean to investigate whether changes in fluxes may have produced the carbonate Sr/Ca variations during each of the studied time intervals. For flux changes resulting from global sea level oscillations, sequence stratigraphic sea level curves can be used to drive the model. For other flux changes, we take an inverse approach, modeling the timing and magnitude of flux changes needed to simulate the timing of Sr/Ca variations observed in the carbonate record. By tracking the Sr isotopic ratio of the ocean, we constrain the magnitude of variations in hydrothermal and continental weathering fluxes which can be invoked to explain carbonate Sr/Ca variations. Finally, we simulate changes in shelf vs. deep sea carbonate sedimentation on seawater Sr/Ca and compare them with the record of reef crises and platform drowning events.

The numerical model is based on one used to investigate the effect of Quaternary glacial sea level changes on Sr and Ca in seawater and is described in detail in Stoll and Schrag (1998); Stoll et al. (1999). Here, we modify the model to investigate long term Sr/Ca variations by including the effect of subsidence of shelf carbonates (at an average rate of 10 m/my; Burke, 1979) and requiring that the carbonate budget balance on timescales > 5000 years. Carbonate, Ca, Sr, and Sr isotopic budgets are started in steady-state for each time interval and remain balanced through $CaCO_3$ compensation, whereby carbonate removal rate adjusts to maintain steady state with respect to carbonate inputs. The parameterization of the Sr and Ca budgets for the Cretaceous ocean, as well as the forcing functions used for model simulations, are detailed in Appendices A and B, respectively.

3.3. Variations resulting from sea level changes

We investigate whether temporal variations in the Sr/Ca ratio of Berriasian–Valanginian, Campanian–Maastrichtian, or sediments of either site in the Albian–Santonian are consistent with those predicted from other indicators of sea level change.

Modeled sea level variations during all intervals produce up to 60% changes in seawater Sr/Ca ratios which are comparable in magnitude to changes observed in the Sr/Ca ratio of carbonates (Fig. 7). Sea level variations driven by the sequence stratigraphic sea level curve produce larger amplitudes of Sr/Ca variation than those driven by oxygen isotopic variations. For the Albian–Santonian, this is because the $\delta^{18}O$ curve, although smoothed, contains many more variations in sea level so that shelf aragonite continuously recycles Sr to the ocean. In contrast, with very infrequent sea level changes represented by the sequence stratigraphic curve, Sr is effectively sequestered in the shelf and large amounts are available for release during sea level falls. In the Berriasian to Valanginian, the lower amplitude response is due to two factors. First, since the sea level was scaled for a total magnitude of 50 m, the individual sea level regressions are lower in magnitude because they are superimposed on long term sea level rise. Secondly, the long-term sea level rise submerges previously deposited shelf carbonates so less carbonate is available for weathering during sea level regressions. This trend is equivalent to a fast subsidence rate.

While sea level changes can cause large variations in the seawater Sr/Ca ratio, the timing and pattern of predicted Sr/Ca variations agrees poorly with the carbonate record. Only for the Campanian–Maastrichtian does the timing of model-predicted Sr/Ca increases correspond well with the measured Sr/Ca ratio increases at the 71 Ma event (Fig. 7c), although model-predicted flux variations cannot reproduce all of the high frequency Sr/Ca variations. In the Albian–Santonian, and perhaps Berriasian–Valanginian where the timing of sea level events may be corroborated by stable isotopic evidence, it is surprising that

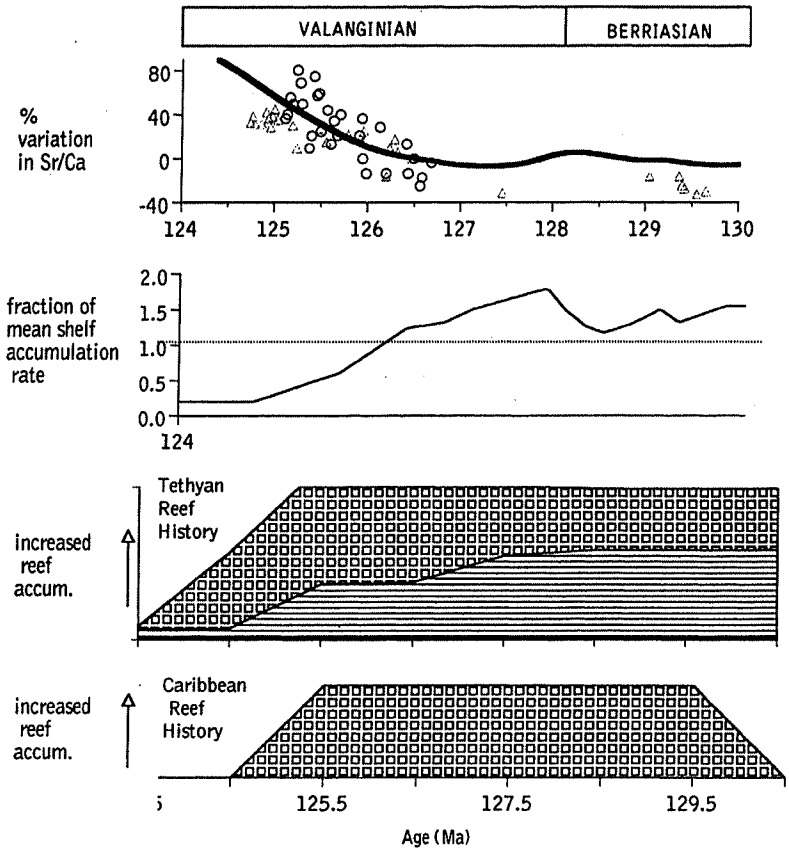

Fig. 8. Variations in deep sea vs. shallow carbonate accumulation as a potential mechanism for carbonate Sr/Ca variations for the Berriasian–Valanginian. Upper panel, carbonate Sr/Ca variation (symbols as in Fig. 2) and model simulated variation in seawater Sr/Ca (thick line). Second panel shows variation in shelf accumulation rate (expressed as a fraction of the mean shelf accumulation rate) which most closely reproduces the observed variation in carbonate Sr/Ca via changes in seawater Sr/Ca. This hypothetical variation in shelf accumulation rate is compared with estimates of Tethyan and Caribbean reef history in the lower panels. Tethyan reef history from Masse and Philip (1981) with age correlation via $\delta^{13}C$ study of Weissert et al. (1998). Caribbean reef history from Kauffman and Johnson, 1988. Brick patterns indicate reef accumulation, horizontal lines indicate littoral sediment accumulation.

the Sr/Ca ratios of carbonates do not record the model-predicted variations. Smaller sea level falls, with superimposed higher frequency sea level oscillations, may have produced Sr/Ca variations which were not as significant compared with other contributions to carbonate Sr/Ca variations.

3.4. Variations resulting from changes in hydrothermal and continental weathering fluxes

Changes in the relative contribution of hydrothermal and continental weathering fluxes affect only slightly on the Sr/Ca ratio of seawater and cannot account for the observed trends in carbonate Sr/Ca ratios because there is little contrast between Sr/Ca ratios of hydrothermal and continental weathering fluxes. Most budgets indicate that the Sr/Ca ratio of the hydrothermal flux is typically twice the Sr/Ca ratio of the continental weathering flux (e.g. Palmer, 1992; Holland, 1984; Meybeck, 1988). Typical changes in the hydrothermal flux can be inferred from estimated ocean crustal generation rates from the Cretaceous (Larson, 1991), since the hydrothermal Sr and Ca fluxes are probably a function of the

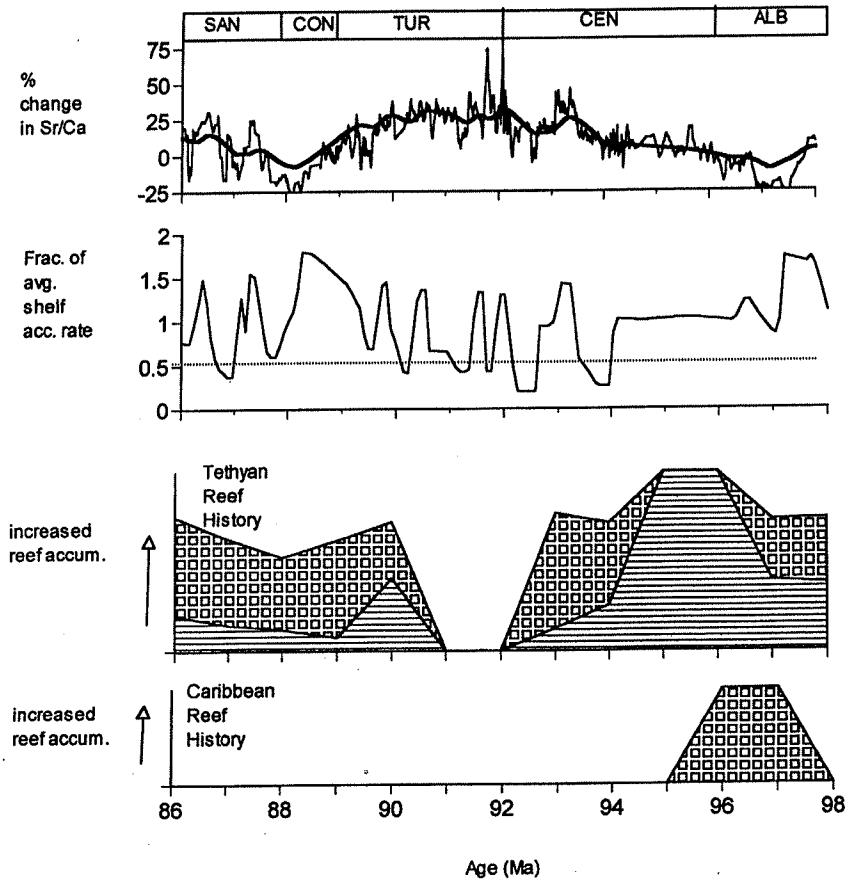

Fig. 9. Variations in deep sea vs. shallow carbonate accumulation as a potential mechanism for carbonate Sr/Ca variations for the Albian–Santonian. Upper panel, carbonate Sr/Ca variation in Contessa Quarry (thin line) and model simulated variation in seawater Sr/Ca (thick line). Second panel shows variation in shelf accumulation rate (expressed as a fraction of the mean shelf accumulation rate) which most closely reproduces the observed variation in carbonate Sr/Ca via changes in seawater Sr/Ca. This hypothetical variation in shelf accumulation rate is compared with estimates of Tethyan and Caribbean reef history in the lower panels. Reef history data as in Fig. 8 except age correlation of Tethyan reef history from Kauffman and Johnson (1988).

hydrothermal fluid flux, which in turn probably varies proportionally to the production rate of new ocean crust. For example, the estimated 30% increase in hydrothermal flux during the Berriasian–Valanginian results in less than 5% increase in seawater Sr/Ca, assuming no change in shelf vs. deep sea carbonate partitioning and constant continental weathering fluxes.

Additional variations in the continental weathering flux (in excess of a factor of two) still produce <5% variations in the Sr/Ca ratio of seawater although they significantly affect its Sr isotopic ratio. Larger variations in the river flux would exceed the limited variations of the Sr isotopic ratio of seawater recorded in carbonate sediments (Jones et al., 1994). Likewise, since the Sr/Ca ratio varies by only a factor of 2–3 among different continental rock types (Meybeck, 1988), changes in the exposure and weathering rate of different rock types change the Sr/Ca ratio of the continental weathering flux only slightly. For example, even a doubling of the relative Ca contribution from igneous and metamorphic rocks, or a 50% increase in the relative contribution from shale and sandstone or evaporites, would change the Sr/Ca

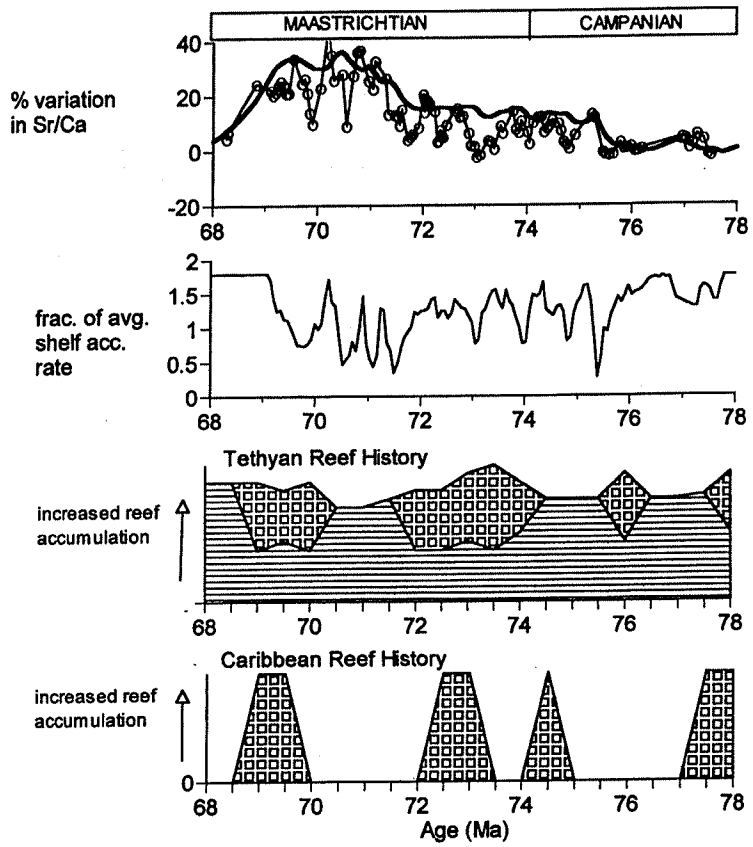

Fig. 10. Variations in deep sea vs. shallow carbonate accumulation as a potential mechanism for carbonate Sr/Ca variations for the Campanian–Maastrichtian. Upper panel, carbonate Sr/Ca variation in DSDP 762C (thin line with points) and model simulated variation in seawater Sr/Ca (thick line). Second panel shows variation in shelf accumulation rate (expressed as a fraction of the mean shelf accumulation rate) which most closely reproduces the observed variation in carbonate Sr/Ca through changes in seawater Sr/Ca. This hypothetical variation in shelf accumulation rate is compared with estimates of Tethyan and Caribbean reef history in the lower panels. Data for lower panels as in Fig. 9.

ratio of the river flux by less than 20% and would not significantly affect seawater Sr/Ca ratios.

3.5. Variations resulting from changing carbonate accumulation in basin vs. shelf environments

Varying the fraction of carbonate removed in shelf vs. deep sea environments can produce variations in seawater Sr/Ca ratios which are comparable to those observed in the carbonate Sr/Ca records, although large changes in shelf accumulation rates are required. In the Berriasian–Valanginian, a 160% decrease in the shelf carbonate accumulation rate (relative to mean accumulation rate) produces an 80% increase in seawater Sr/Ca over several million years (Fig. 8). In the Upper Cretaceous, where shelf carbonates consist of a mixture of aragonite and calcite, comparable variations in shelf accumulation rates produce only 40% variations in seawater Sr/Ca (Figs. 9 and 10). For all intervals, these variations might account for a significant portion of the variation in carbonate seawater Sr/Ca ratios over periods of 1 Ma or more, but cannot reproduce the higher frequency variations due to the long residence times of Sr and Ca in the ocean.

While it is difficult to assess whether the magnitude of these variations in shelf accumulation rate is reasonable, we can evaluate whether the timing of

the required variations in shelf accumulation rate are consistent with other data. Several factors may influence the proportion of carbonate accumulating in shelf vs. deep sea environments, including imbalances in the carbonate budget which are compensated by changes in the carbonate compensation depth (CCD), area of shelf habitat, and environmental conditions in shelf habitats. The magnitude of changes in the carbonate influx from continental weathering and hydrothermal exchange is constrained by the isotopic ratio of seawater to be no larger than a factor of 2. If all of the changes in influx were compensated via deep sea carbonate accumulation, the resulting variations in the Sr/Ca ratio of seawater would be less than 10%, not sufficient to explain the variation in carbonate Sr/Ca for any time period.

Short term changes in the area of shallow shelf carbonate accumulation most likely result from sea level changes, and the magnitude of the reduction will depend on the coastal hypsometry at the time of sea level fall. For example, including a 50% reduction in the shelf carbonate accumulation rate during Campanian–Maastrichtian sea level falls increases the amplitude of Sr/Ca variations by 15% (Fig. 7(c)). However, as discussed above, the timing of sea level falls corresponds poorly to Sr/Ca variations during most intervals so basin/shelf fractionation due to sea level falls is not likely to explain the observed carbonate Sr/Ca variations.

The carbonate production of shelf organisms can vary with factors other than the area of habitat within a suitable depth range. For Cretaceous reef builders, various 'reef crisis' have been described when carbonate platform demise may result from changes in temperature (Johnson et al., 1996), and nutrient levels and turbidity (Weissert et al., 1998). The relative timing of the Valanginian reef crisis in the Tethyan is well constrained by the $\delta^{13}C$ excursion measured in reef and deep sea carbonates (Weissert et al., 1998) permitting precise correlation with our records. A short burst of reef development in the Caribbean also ends in the Middle Valanginian (Kauffman and Johnson, 1988). While these decreases in reef carbonate accumulation may in part explain ascending carbonate Sr/Ca ratios, the decrease in reef carbonate accumulations post-date the ascent in Sr/Ca ratios, suggesting that other factors also contributed to the ascent in carbonate Sr/Ca ratios (Fig. 8).

Agreement between modeled variations in shelf carbonate production and observed reef accumulation is variable during the Upper Cretaceous intervals and is more difficult to assess because of uncertainties in correlation. A reef crisis at the Cenomanian–Turonian boundary in Tethyan sections corresponds with generally lower shelf accumulation rates required by the model, although the Late Cenomanian demise of reef carbonates postdates the decline required by the model (Fig. 9). By the Campanian/Maastrichtian interval, reef growth was sporadic in both the Tethys and Caribbean. It is difficult to determine if the rapid model-required variations in shelf accumulation rate are consistent with reef history from 78 to 72 Ma (Fig. 10). However, the model-required decline in shelf carbonate accumulation rate between 72 and 70 Ma appears to be reflected in the cessation of reef accumulation in both the Tethys and Caribbean.

3.6. Summary of modeling results

Rapid sea level falls may explain the overall increases in Sr/Ca at 71 Ma and possibly 75 Ma, but do not appear to explain the pattern of Sr/Ca variations in either the Berriasian–Valanginian or Albian–Santonian intervals. Changes in the fraction of carbonate sedimentation accumulated in shelf vs. deep sea settings represent the most likely source of variations in seawater Sr/Ca ratios which might explain some of the observed variations in the Sr/Ca ratios of Cretaceous carbonates. In the Early Maastrichtian, Cenomanian–Turonian boundary, and in the Valanginian, the timing of some reef crises is consistent with increased Sr/Ca ratios due to decreased shelf accumulation rates. However, we cannot asses whether the magnitude of changes in shelf carbonate accumulation rates is reasonable. Furthermore, basin-shelf fractionation cannot explain all of the variations. In the Berriasian–Valanginian, where the timing of such events is tightly constrained, reef crises postdate the beginning of the ascent of Sr/Ca ratios and cannot be the only cause of increasing Sr/Ca. In the Upper Cretaceous, no flux changes can reproduce the rapidity of some of the changes in carbonate Sr/Ca ratios. If the timescale of the most rapid changes in carbonate Sr/Ca is not biased by changing sedimentation rates and/or diagenesis, then other factors must cause these changes. We conclude that while sea level changes

and basin-shelf fractionation likely contributed to variation in seawater Sr/Ca ratios it was not the only source, and probably not even the dominant source, of variations in carbonate Sr/Ca.

4. Evaluating variations in Sr partitioning: response to productivity changes?

4.1. Controls of Sr partitioning in modern nannofossil carbonate

Since changes in Sr fluxes to the ocean do not appear to be able to explain the magnitude and timescale of many Sr/Ca variations in Cretaceous carbonates, we consider how changes in Sr partitioning in these carbonates may have been an important control over their Sr/Ca ratios. All of the sediments studied are dominated to a high degree by coccolith or calcareous nannofossil carbonate (>90% of carbonate in Contessa sediments is from coccoliths (Arthur, 1979); in 762C the percentage is also very high (Exon et al., 1992). Recent studies indicate that across modern upwelling systems, Sr partitioning in nannofossil carbonate parallels variations in coccolithophorid productivity, calcification, and growth rate (Stoll and Schrag, 2000b; Stoll et al., 2000). Bulk carbonate Sr/Ca variations are driven by changing coccolithophorid Sr/Ca and higher contributions of coccolith carbonate (Sr/Ca 2–2.5 mmol/mol) relative to foraminiferal carbonate (1.2–1.4 mmol/mol) in areas of maximum upwelling intensity (Stoll and Schrag, 2000b). Culture studies of a number of coccolithophorid species also demonstrate increased Sr partitioning with increased cell division rate and calcification rate (Stoll et al., 2000; Rosenthal et al., 2000; Stoll et al., in review). Across upwelling systems and in culture studies, Sr/Ca typically varies by 15–25%. The magnitude of the temporal variations in Sr/Ca of Cretaceous sediments is a factor of 2 larger than observed across the modern productivity gradients in upwelling regions. Temporal changes in species assemblages and a wider range in calcification rates may cause larger amplitude variations.

4.2. Other indicators of productivity from microfossil ecology

To evaluate the possibility that productivity changes drove variations in Sr partitioning in Cretaceous carbonates, we compare Sr/Ca data with other indicators of marine productivity. For the Upper Cretaceous, Premoli-Silva and Sliter (1994) have distinguished species of planktonic foraminifera which likely followed life strategies of r-, K-, and intermediate selection. K-selected taxa show specializations adapted to stable but difficult (resource-poor) environments, whereas r-selected taxa are opportunists adapted to rapid exploitation of resource-rich environments (e.g. Guillard and Kilham, 1977; Margalef, 1978). In the data of Premoli Silva and Sliter (1994), the fractions of both r-selectors and intermediate species are anticorrelated to the fractions of k-selectors and are interpreted as representing high productivity assemblage. We use the percent of r + intermediate species as one indicator of productivity changes in Upper Cretaceous sections. Ideally, we would like to compare microfossil productivity indices with Sr/Ca data from the same site. High-resolution planktonic foraminiferal data for the Upper Cretaceous of Gubbio (Premoli Silva and Sliter, 1994) overlap with our Albian to Santonian record from the Contessa Quarry in Gubbio. However, we are not aware of published microfossil census data for any of the DSDP sites in this study. Data on % r + intermediate were compiled for each biozone by Premoli-Silva and Sliter (1994). To compare data at higher temporal resolution, we additionally have calculated a % r + I index for each sample level from the species abundance data of Premoli-Silva and Sliter (1994).

Indicators of calcareous nannoplankton productivity have also been studied in Cretaceous sediments. Several groups have recognized a high fertility assemblage (consisting of *Biscutum constans*, *Zygodiscus (Zeugrhabdotus) elegans* and *Z. erectus*, and *D. ignotus* (e.g. Roth and Krumbach, 1986; Premoli-Silva et al., 1989; Watkins, 1989). Nannoconids have been distinguished as characteristic of oligotrophic to mesotrophic environments, whereas *W. barnesiae* is inferred to reflect high fertility surface waters (Tremolada et al., 1999, 2000; Erba et al., 1994). Although quantitative application of this scheme is difficult since only a few species have been characterized (whereas all species are characterized with the foraminiferal r + intermediate index), we can examine changes in the abundance of high productivity

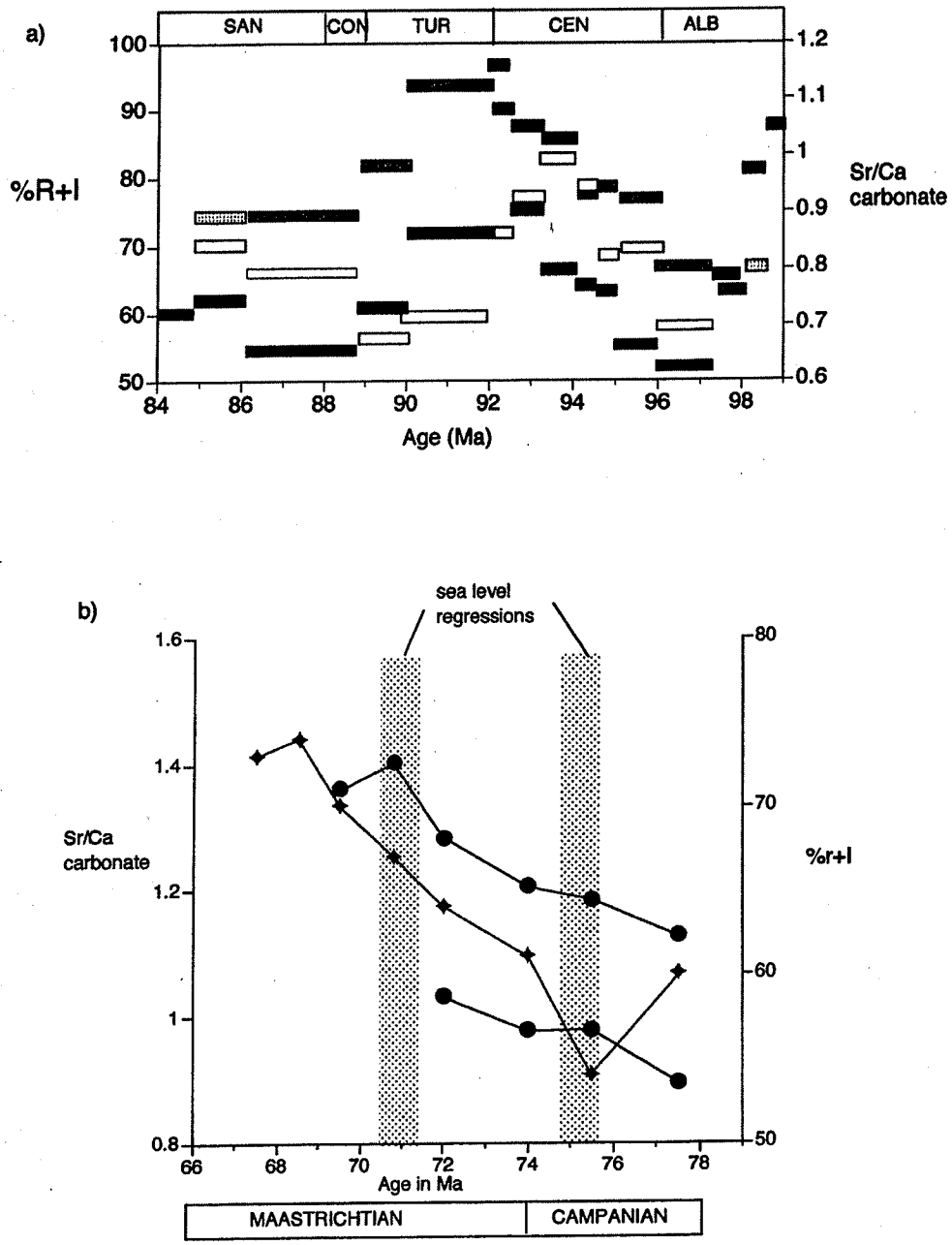

Fig. 11. Relation of carbonate Sr/Ca with other indices of productivity for Upper Cretaceous, data averaged for each biozone. Comparison of carbonate Sr/Ca with paleoecological productivity index (%r + I planktonic foraminifera, described in Section 4.2). (a) Data from Albian–Santonian interval. Black squares, % r + I; grey squares, Sr/Ca data from Contessa Quarry; white squares, Sr/Ca data from Santa Ines. (b) Data from Campanian–Maastrichtian interval, plotted at midpoint of biozone. Open squares, % r + I; filled circles, Sr/Ca data from DSDP 762C; open circles, data from DSDP 516F. The timing of sea level regressions is indicated by shaded areas. For both panels, %r + I plantonic foraminiferal index calculated by Premoli-Silva and Sliter (1994).

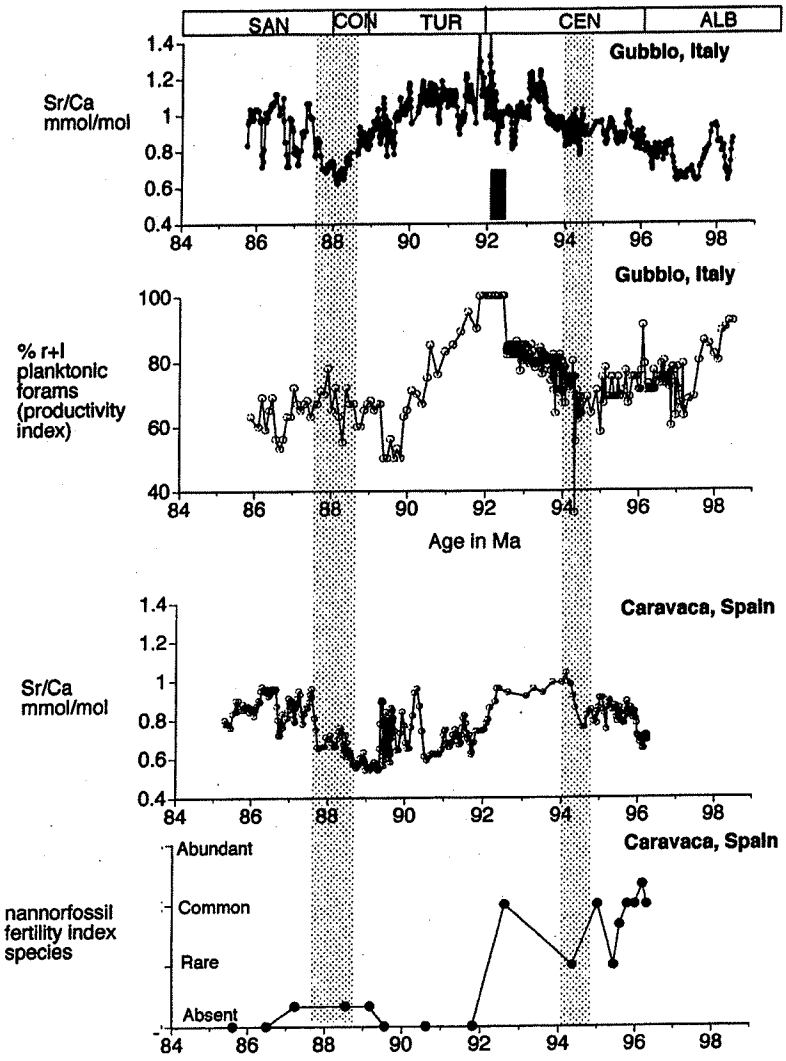

Fig. 12. Relation of carbonate Sr/Ca with site-specific indices of productivity for Albian–Santonian interval. %r + I plantonic foraminiferal index calculated from data of Premoli-Silva and Sliter (1994)and nannofossil fertility index calculated from data of Aguado (1994), as detailed in Section 4.2 of the text. Shaded bars indicate sea level regressions (from $\delta^{18}O$ record) and potentially elevated seawater Sr/Ca. The black rectangle at 92.5 Ma in the upper panel denotes the black shales of the Bonarelli Horizon.

assemblages. Detailed nannofossil data have been compiled for the Santa Ines section in Spain (Aguado, 1994). Nannofossil data are also available for the Campanian–Maastrichtian of Italian sections (Monechi and Thierstein, 1985); however, many of the index species for productivity are absent. Further studies of nannofossil paleoecology in the latest Cretaceous are probably needed in order to interpret productivity changes from nannofossil assemblages. Detailed work on the abundance of nannoconids and productivity changes for Lower Cretaceous sections in Italy has been undertaken by Erba et al. (1994) and Tremolada and Erba (2000) which we summarize and compare with our geochemical data.

4.3. Comparing Upper Cretaceous carbonate Sr/Ca with ecologic productivity indicators

For the Albian to Santonian where microfossil and Sr/Ca data are both available for the Gubbio site, Sr/Ca and the % r + I index show broadly similar patterns of variation (Fig. 11a). Both increase significantly during the Cenomanian and decrease through the Turonian and Coniacian, and are relatively stable through the Lower Santonian. This similarity may reflect generally synchronous productivity changes in planktonic foraminifera and calcareous nannofossils over this timescale, perhaps due to changes in some factor that increased the overall productivity of the environment. Because the Sr/Ca ratio of the Santa Ines record differs from that of the Italian section, it does not show as strong a correlation with the % r + I index from the Italian site. In the Santa Ines section of Spain, Sr/Ca ratios increase through the Lower and Middle Cenomanian but decrease earlier than the % r + I index from the Italian section. It is possible that this divergence reflects differences in the productivity between the two sites, a possibility that we subsequently discuss in light of the nannofossil-based productivity index for the Santa Ines section. For the Campanian–Maastrichtian, the % r + I index from Italy and Sr/Ca records from site 516F in the South Atlantic and from 762C in the Indian Ocean show similar increases from the Upper Campanian through the Lower Maastrichtian (Fig. 11b). Two biozones with opposing patterns in Sr/Ca and %r + I at 75 and 71 Ma correspond to sea level regressions, and at 71 Ma to reduced reef accumulation. Both of these factors may have contributed to higher seawater Sr/Ca and hence higher carbonate Sr/Ca relative to constant or decreasing productivity.

Comparing the data at higher resolution indicates that in the Upper Albian–Santonian, there are broadly similar variations in foraminiferal paleoproductivity estimates and Sr/Ca variations, as suggested by the biozone averages (Fig. 12). Both records indicate high productivity at the time of deposition of the black shales of the Bonarelli Horizon (92.5 Ma). These and other black shale events are believed to result from increased fertility and concomitant production of organic matter which produced sediment anoxia. Both microfossil ecology and carbonate Sr/Ca suggest gradual, rather than abrupt, increases in productivity leading up to the black shales of the Bonarelli Horizon at 92.5 Ma. Gradual productivity increases leading up to the deposition of analogous black shales of the Selli Horizon (Aptian) have also been inferred from nannofossil ecology (Tremolada and Erba, 2000).

The most prominent difference between Sr/Ca and ecological productivity indices in the Gubbio section is the earlier decline in productivity after the maxima at the Cenomanian/Turonian boundary compared to the much later decline in Sr/Ca in the Contessa section. Foraminiferal productivity is also relatively stable during the Coniacian and Santonian whereas Sr/Ca increases in both Contessa and Santa Ines records. These discrepancies cannot be readily explained by changes in seawater Sr/Ca ratios due to sea level changes, because the Turonian–Coniacian sea level falls would increase Sr/Ca ratios during this interval. One possibility is that Sr partitioning is also affected by temperature, although temperature was not the dominant control over Sr/Ca ratios in core top samples across the equatorial upwelling zone (Stoll and Schrag, 2000b). Interestingly, positive excursions in the oxygen isotopic record of the Contessa section at 95–94 and 89–90 Ma indicate cooler temperatures which correspond to negative excursions in the foraminiferal productivity index but not to negative excursions in Sr/Ca. An alternative explanation for the discrepancies between foraminiferal productivity and Sr/Ca at shorter timescales is that the productivity of planktonic foraminifera and calcareous nannoplankton may be decoupled because they may have different factors limiting their growth rates.

For the Santa Ines section, high-fertility (nannofossil) indicators *Z. noellae*, *B. constans* and *D. ignotus* occur in the Albian to Cenomanian and then disappear in the Upper Cenomanian. The disappearance of these species coincides with the rapid drop in Sr/Ca ratios in this section in the Upper Cenomanian (Fig. 12). This may indicate that productivity variations were not synchronous in the Santa Ines and Contessa sections (or that stratigraphic complexities in the Santa Ines section precludes correlation at high resolution). However, increases in Sr/Ca in the Upper Turonian and Lower Santonian are only matched by the return of rare *D. ignotous*, although the stratigraphic ranges of all three species extend beyond the Santonian.

Detailed comparisons of foraminiferal ecology and

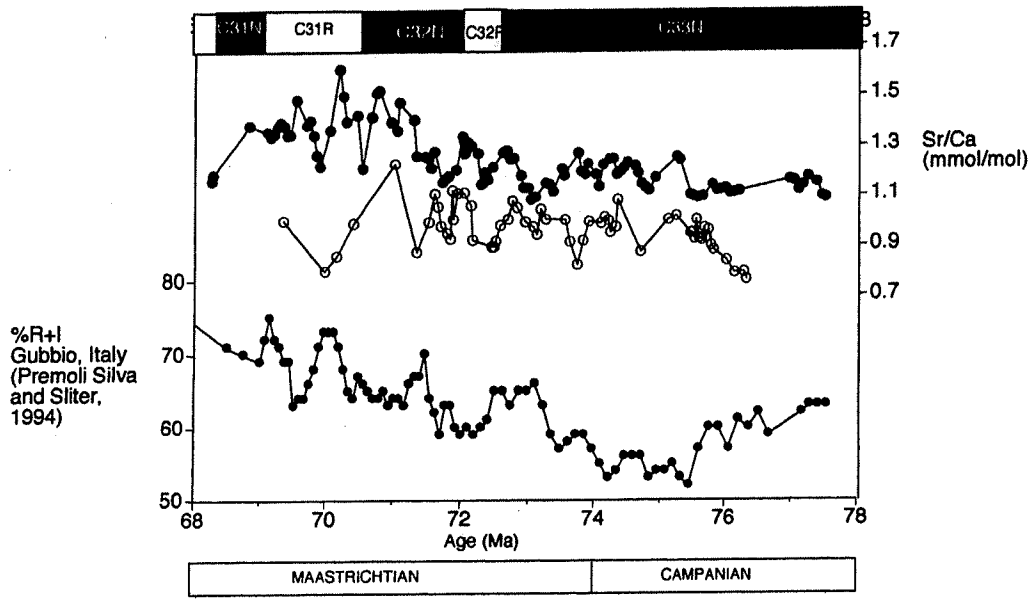

Fig. 13. Detailed comparison of carbonate Sr/Ca with indices of productivity for Campanian–Maastrichtian interval. %r + I plantonic foraminiferal index calculated from data ofPremoli-Silva and Sliter (1994). Sr/Ca data as in Fig. 6; Open circles, site 516F; closed circles, site 762C.

Sr/Ca for the Campanian–Maastrichtian show that numerous small excursions in Sr/Ca may correspond to excursions in the foraminiferal productivity index, especially from 70.5 to 69 Ma (Fig. 13). Because the correlation is imprecise during the C33N magnetochron, it is difficult to establish whether the small variations in productivity and Sr/Ca correspond during this time; for example, peaks at 73 Ma and the minima between 72.5 and 72.0 may correspond. At 71.5 Ma, Sr/Ca ratios ascend rapidly with little change in the foraminiferal productivity index. This increase may be due in part to increased seawater Sr/Ca ratios due to the sea level regression and possibly reef demise at this time. Differences may also result from different ecological responses of calcareous nannoplankton and foraminifera and from local productivity variations, since the foraminiferal productivity data are from the Tethys but the Sr/Ca data are from the South Atlantic and Indian Oceans.

4.4. Comparing Lower Cretaceous carbonate Sr/Ca with ecologic productivity indicators

For the Berriasian–Valanginian time interval, the abundance of oligotrophic nannoplankton (nannoconids) decreases and the abundance of high surface water fertility assemblages (*W. barnesiae*) increases, beginning 1–2 m.y. prior to the initiation of the positive $\delta^{13}C$ excursion (Tremolada and Erba, 2000). The timing of this hypothesized increase in productivity of surface waters corresponds well with the increase in Sr/Ca (Fig. 14). The $\delta^{13}C$ increase itself has been interpreted as reflecting increased surface water fertility (Weissert et al., 1998). Weissert et al. (1998) argue that intensified volcanic activity (Parana Flood Basalts) enhanced greenhouse conditions and accelerated hydrological cycling, leading to greater weathering and nutrient influx. Higher nutrient flux is also supported by increased P accumulation rates in sediments, and the timing of the P increase also corresponds well to the Sr/Ca increase (Fig. 14; Follmi, 1995). Consequently, the increased Sr/Ca ratio is likely to reflect increased Sr partitioning, possibly due to faster growth rates of r-selecting calcareous nannofossils which would thrive in higher productivity environments and which tend to be growth-rate maximizing (Young, 1994).

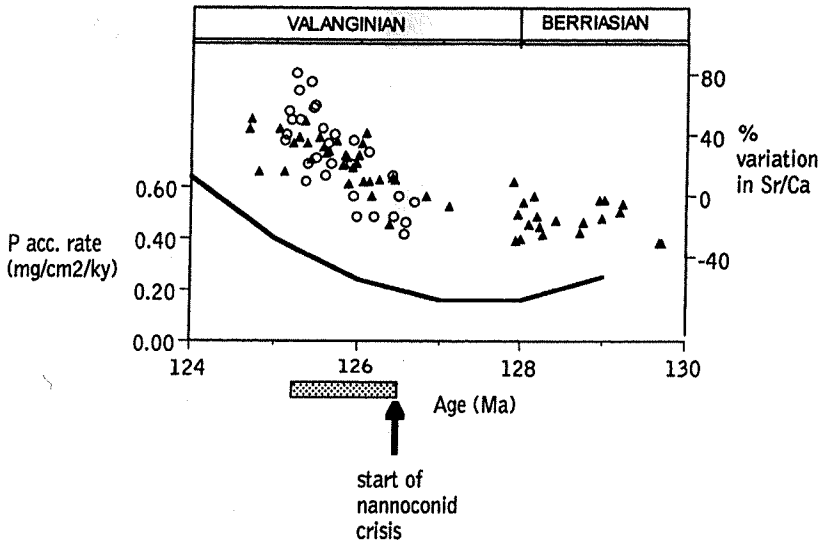

Fig. 14. Relation of carbonate Sr/Ca with other indices of productivity for the Berriasian–Valanginian. Sr/Ca data (symbols, as in Fig. 2) and PO_4 accumulation rate data of Follmi (1995; thick line). Below, arrow and shaded box denote beginning of nannoconid decline (decline of oligotrophic calcareous nannofossils) and hypothesized increase of surface water fertility described by Erba (1994); Tremolada and Erba (2000).

4.5. Summary of likely variations in Sr partitioning

Taken as a whole, these observations suggest that productivity-related influences on Sr partitioning in carbonates is significant. Changes in surface nutrient concentrations and nannoplankton ecology provide the best temporal match to changes in carbonate Sr/Ca ratios in the Valanginian. The nannoplankton productivity record inferred from the Santa Ines section provides the best explanation for the differences in Sr/Ca variations between the Albian–Santonian records from Italy and Spain. The different patterns of Sr/Ca variation in the Albian–Santonian records cannot be due to changes in seawater Sr/Ca ratios that are globally uniform. Overall patterns of Sr/Ca variation correspond well to ecological productivity indices and models for black shale development in the Albian–Santonian record at Gubbio. Furthermore, some large and very rapid Sr/Ca variations in the Early Maastrichtian records correspond with rapid changes in the foraminiferal productivity index. Such large rapid changes cannot be explained by flux changes. Similarity between foraminiferal productivity records in Italy and Sr/Ca records from the Indian Ocean and South Atlantic ocean may indicate that some of the Maastrichtian productivity variations were global, perhaps tied to changes in nutrient flux and thermohaline circulation (Barrera et al., 1997).

5. Conclusions

High resolution Sr/Ca measurements on coccolith-dominated pelagic carbonates of Berriasian–Valanginian, Albian–Santonian, and Campanian–Maastrichtian age from DSDP sites and Tethyan land sections indicate large variations (up to 80%) in Sr/Ca both over long and short timescales. Models of seawater Sr/Ca and compilation of ecological productivity indices suggest that changes in Sr partitioning, likely due to changes in calcareous nannoplankton productivity, are the dominant control over varying carbonate Sr/Ca in these records. However, model results indicate that sea level changes and reef crisis events could produce significant variations in seawater Sr/Ca through time. Fortunately, the influence of sea level changes on seawater Sr/Ca (both through reef weathering and reef crises) can often be constrained from independent geological data, and

isotopic ratio of the continental weathering flux has probably not changed significantly from 140 to 40 Ma, since the long term trends in seawater Sr isotopes can be well explained by the changing contribution of hydrothermal and continental weathering fluxes due changes in ocean crust production alone. We begin each model simulation with the $^{87}Sr/^{86}Sr$ ratio of the ocean equal to that measured in carbonates (Jones et al., 1994), and set the proportion of Sr flux from river and hydrothermal sources to be in steady state with the $^{87}Sr/^{86}Sr$ of the ocean. The proportion of Ca flux from hydrothermal vs. continental weathering is adjusted to maintain a constant factor of ≈ 2 difference between Sr/Ca ratios of continental weathering and hydrothermal sources.

Appendix B. Forcing models of seawater Sr/Ca with Cretaceous sea level changes

Records of eustatic sea level changes from sequence stratigraphy (Haq et al., 1987) are used to drive the model for all time periods. One limitation is the difficulty in precise correlation of the sequence stratigraphy with our geochemical data, particularly for the older time intervals. For the Berriasian–Valanginian and Upper Albian–Santonian, the geochemical records must be correlated with the sea level curve via biostratigraphy, which may have uncertainties of 1–2 m.y. The correlation may be more accurate for the Berriasian–Valanginian where magnetostratigraphy improves the stratigraphic framework of the sea level curve. For the Campanian–Maastrichtian intervals, magnetostratigraphy provides a more precise correlation with the sequence stratigraphic sea level curve.

For the Upper Albian–Santonian, the $\delta^{18}O$ record from these sites may provide an alternative sea level record without problems of correlation. In these sites, the pattern of large positive excursions in $\delta^{18}O$, as well as the periods of relatively stable $\delta^{18}O$, closely resembles the pattern of sea level change in the sequence stratigraphic record. Within the uncertainty of biostratigraphic correlation, the largest positive $\delta^{18}O$ excursions correspond to major sea level regressions in the stratigraphic sea level curve. We have previously demonstrated that these variations are not likely to result from diagenesis and may indicate glacioeustatic control of sea level (Stoll and Schrag, in press). Although the $\delta^{18}O$ record is likely to vary in response to both temperature and sea level changes, we assume that the relative contribution of each effect remains constant throughout the record and that the $\delta^{18}O$ record thus approximately reproduces the timing and relative magnitude of sea level changes. We drive the model both with a smoothed $\delta^{18}O$ record from the Contessa Quarry section and a smoothed composite $\delta^{18}O$ record from both sections. We also apply this approach in the Berriasian–Valanginian, using a smoothed $\delta^{18}O$ record from site 534A which shows two $\delta^{18}O$ excursions whose timing roughly coincides with regressions in the sequence stratigraphic curve (Haq et al., 1987). For the Campanian–Maastrichtian, oxygen isotopic data from our sites show trends which do not appear to be related to sea level changes. Although Barrera et al. (1997)identified a significant positive excursion in oxygen isotopes between 71 and 70 Ma which corresponds to a sea level regression in the sequence stratigraphic curve (Haq et al., 1987), we cannot discern this event in our record.

Although the timing of sea level change is set by available records, the magnitude of the resulting response in seawater Sr/Ca is dependent on several model parameter choices. Large magnitudes of the sea level change, low rates of shelf subsidence, extensive shelf aragonite recrystallization, and limited dissolution of shelf carbonates maximize the amplitude of Sr/Ca variations. We scale all sea level curves to produce maximum sea level variations of 50 m, and use a moderate subsidence rate of 10 m/my, assuming that 70% of all aragonite recrystallizes within a hundred thousand years of exposure and that the dissolution flux of shelf carbonates is at most 30% of the average carbonate accumulation rate during maximum exposure (see Stoll and Schrag, 1998 for a detailed discussion of these parameter choices). Sensitivity experiments indicate that these parameter choices produce conservative estimates of the effect of sea level changes on seawater Sr/Ca, and that the magnitude of the response may vary by a factor of two for any given sea level forcing.

References

Aguado, R., 1994. Nannofosiles del Cretacico de la Cordillera Betica (Sur de Espana): Bioestratigrafia. Doctoral, Granada.
Apitz, S. E., 1991. The lithification of ridge flank basal carbonates:

Characterization and implications for Sr/Ca and Mg/Ca in marine chalks and limestones. PhD, University of California, San Diego.

Arthur, M.A., Fisher, A.G., 1977. Upper Cretaceous–Paleocene magnetic stratigraphy at Gubbio, Italy, I. Lithostratigraphy and sedimentology: GSA Bulletin 88, 367–389.

Arthur, M.A., 1979, Sedimentologic and geochemical studies of Cretaceous and Paleogene pelagic sedimentary rocks. PhD dissertation, Princeton, Princeton University.

Arthur, M.A., Dean, W.E., Claypool, G.E., Scholle, P.A., 1985. Comparative geochemical and mineralogical studies of two cyclic transgressive pelagic limestone units, Cretaceous Western Interior Basin, U.S. In: Pratt, L.M., Kauffman, E.G., Zelt, F.B. (Eds.), Fine Grained Deposits and Biofacies of the Cretaceous Western Interior Seaway: Evidence for Cyclic Sedimentary Processes S.E.P.M. Field Guidebook.

Barrera, E., Savin, S., Thomas, E., Jones, C.E., 1997. Evidence for thermohaline-circulation reversals controlled by sea-level change in the latest Cretaceous. Geology 25, 715–718.

Berggren, W.A., Hamilton, N., Johnson, D.A., Pujol, C., Weiss, W., Cepek, P., Gombos, A.M., 1989. Magnetobiostratigraphy of deep sea drilling project Leg 72, Sites 515-518, Rio Grande Rise (South Atlantic). In: Barker, P.F., Carlson, R.L., Johnson, D.A. (Eds.), Init. Repts. DSDP, 72: Washington (US Govt. Printing Office).

Bralower, T.J., Siesser, W.G., 1992. Cretaceous calcareous nannofossil biostratigraphy of sites 761, 762, and 763, Exmouth and Wombat Plateaus, Northwest Australia. In: von Rad, U., Haq, B.U. (Eds.), Proceedings of the Ocean Drilling Program, Scientific Results. College Station, Texas: Ocean Drilling Program, pp. 529–547.

Bralower, T.J., Moneci, S., Thierstein, H.R., 1989. Calcareous nannofossil zonation of the Jurassic–Cretaceous boundary interval and correlation with the geomagnetic polarity timescale. Marine Micropaleontology 14, 153–235.

Burke, K., 1979. The edge of the ocean: an introduction. Oceanus 22, 3–11.

Erba, E., 1994. Nannofossils and "superplumes": the Early Aptian nannoconid crisis. Paleoceanography 3, 483–501.

Exon, N.F., Borella, P.E., Ito, M., 1992. Sedimentology of Cretaceous sequences in the Central Exmouth Plateau. In: Von Rad, U., Haq, B.U. (Eds.), Proceedings of ODP, Scientific. Results 122: College Station, Texas, pp. 233–254.

Follmi, K.B., 1995. 160 m.y. record of marine sedimentary phosphorus burial: coupling of climate and continental weathering under greenhouse and icehouse conditions. Geology 23, 859–862.

Galbrun, 1992. Magnetostratigraphy of Cretaceous sequences. In: Von Rad, B.,Haq, B.U. (Eds.), Proceedings of ODP, Scientific Results 122. College Station, Texas.

Graham, D.W., Bender, M.L., Williams, D.F., Keigwin Jr, L.D., 1982. Strontium-calcium ratios in Cenozoic planktonic foraminifera. Geochimica et Cosmochimica Acta 46, 1281–1292.

Guillard, R.R.L., Kilham, P., 1977. The ecology of marine planktonic diatoms. In: Werner, D. (Ed.), The Biology of Diatoms. Blackwell Scientific Publications, Oxford, pp. 372–469.

Haq, B., Hardenbol, J., Vail, P., 1987. Chronology of fluctuating sea levels since the Triassic. Science 23, 1156–1167.

Holland, H.D., 1984. The Chemical Evolution of the Atmosphere and Oceans. Princeton University Press, New Jersey.

Johnson, D.A. 1984. Paleocirculation of the Southwestern Atlantic. In Barker, P.F., Carlson, R.L., Johnson, D.A. (Eds.), Init. Repts. DSDP, 72: Washington (US Govt. Printing Office).

Johnson, C., Barron, E.J., Kauffman, E.G., Arthur, M.A., Fawcett, P.J., Yasuda, M.K., 1996. Middle Cretaceous reef collapse linked to ocean heat transport. Geology 24, 376–380.

Jones, C.E., Jenkyns, H.C., Coe, A.L., Hesselbo, S.P., 1994. Strontium isotopic variations in Jurassic and Cretaceous seawater. Geochim. et Cosmochim. Acta 58, 3061–3074.

Kauffman, E.G., Johnson, C.C., 1988. The morphological and ecological evolution of Middle and Upper Cretaceous reef-building rudistids. Palaios 3, 194–216.

Kuhnt, W., 1990. Agglutinated foraminifera of western Mediterranean Upper Cretaceous pelagic limestones (Umbrian Apennines, Italy, and Betic Cordillera, Southern Spain). Micropaleontology 36, 297–330.

Larson, R.L., 1991. Latest pulse of Earth: Evidence for a mid-Cretaceous superplume. Geology 19, 547–550.

Lini, A., Weissert, H., Erba, E., 1992. The Valanginian carbon isotope event: a first episode of greenhouse climate conditions during the Cretaceous. Terra Nova 4, 374–384.

Margalef, R., 1978. Life forms of phytoplankton as survival alternatives in an unstable environment. Oceanol. Acta 1, 493–509.

Masse, J.P., Philip, J., 1981. Cretaceous coral-rudist buildups in France. In: D. F. Toomly (Ed.), European fossil reef models. Society of Economic Paleontologists and Mineralogists Special Publication 30, pp. 399–426.

Meybeck, M., 1988. Sr/Ca ratios in rivers. In: Letman, A.M. (Ed.), Physical and Chemical Weathering in Geochemical Cycles, p. 261.

Monechi, S., Thierstein, H.R., 1985. Late Cretaceous–Eocene nannofossil and magnetostratigraphic correlations near Gubbio. Italy. Marine Micropaleontology 9, 419–440.

Opdyke, B.N., Wilkinson, B.H., 1988. Surface area control of shallow cratonic to deep marine carbonate accumulation. Paleoceanography 3 (6), 685–703.

Palmer, M.R., 1992. Controls over the chloride concentration of submarine hydrothermal vent fluids: evidence from Sr/Ca and 87Sr/86Sr ratios. Earth and Planetary Science Letters 109, 37–46.

Premoli Silva, I., Sliter, W.V., 1994. Cretaceous planktonic foraminiferal biostratigraphy and evolutionary trends from the Bottaccione section, Gubbio, Italy. Palaeontographia Italica 82, 1–89.

Premoli Silva, I., Erba, E., Tornaghi, M.E., 1989. Paleoenvironmental signals and changes in surface fertility in mid Cretaceous Corg-righ pelagic facies of the fucoid marls (central Italy). Geobios. Mem. Spec. 11, 225–236.

Renard, M., 1986. Pelagic Carbonate Chemostratigraphy. Marine Micropaleontology 10, 117–164.

Richter, F.M., DePaolo, D.J., 1987. Numerical models for diagenesis and the Neogene Sr isotopic evolution of seawater from DSDP Site 590B. Earth and Planetary Science Letters 83, 27–38.

Richter, F.M., DePaolo, D.J., 1988. Diagenesis and Sr isotopic evolution of seawater using data from DSDP 590B and 575. Earth and Planetary Science Letters 90, 382–394.

Richter, F.M., Liang, Y., 1993. The rate and consequences of Sr diagenesis in deep-sea carbonates. Earth and Planetary Science Letters 117, 553–565.

Richter, F.M., 1996. Models for the coupled Sr-sulfate budget in deep-sea carbonates. Earth and Planetary Science Letters 141, 199–211.

Rosenthal, Y., Stoll, H.M., Wyman, K., Falkowski, P. Growth Related Variations in Carbon Isotopic Fractionation and Coccolith Chemistry in Emiliania huxleyi. AGU/ASLO Ocean Sciences Meeting (San Antonio, Texas), January 2000.

Roth, P.H., Krumbach, K.R., 1986. Middle Cretaceous nannoplankton biogeography and preservation in the Atlantic and Indian oceans: implications for paleoceanography. Marine Micropaleontology 10, 235–266.

Schlanger, S.O., 1988. Strontium storage and release during deposition and diagenesis of marine carbonates related to sea-level variations. In: Lerman, A., Meybeck, M. (Eds.), Physical and Chemical Weathering in Geochemical Cycles. Kluwer, Boston, pp. 323–340.

Schlanger, S.O., Douglass, R.G., 1974. The pelagic ooze-chalk-limestone transition and its implications for marine stratigraphy. Spec. Publs. Int. Assoc. Sediment. 1, 117–148.

Schrag, D.P., DePaolo, D.J., Richter, F.M., 1995. Reconstructing past sea surface temperatures: correcting for diagenesis of bulk marine carbonate. Geochimica et Cosmochimica Acta 59, 2265–2278.

Scott, R.W., 1988. Evolution of Late Jurassic and Early Cretaceous Reef Biotas. Palaios, 184–193.

Shackleton, N.J., Hall, M.A., Pate, D., Meynadier, L., Valet, P, 1993. High-resolution stable isotope stratigraphy from bulk sediment. Paleoceanography 8, 141–148.

Stoll, H.M., Schrag, D.P., 1996. Evidence for glacial control of rapid sea level changes in the Early Cretaceous. Science 272, 1771–1774.

Stoll, H.M., Schrag, D.P., 1998. Effects of Quaternary sea level changes on strontium in seawater. Geochim. Cosmochim. Acta 62, 1107–1118.

Stoll, H.M., Schrag, D.P., 2000a. High resolution stable isotope records from the Upper Cretaceous of Italy and Spain: glacial episodes in a greenhouse planet? GSA Bulletin 112, 308–319.

Stoll, H.M., Schrag, D.P., 2000b. Coccolith Sr/Ca as a new indicator of coccolithophorid calcification and growth rate. Geochemistry Geophysics Geosystems, 1.

Stoll, H.M, Klaas, C., Probert, I., Ruiz-Encinar, J., Garcia-Alonso, J.I., 2001. Calcification rate and temperature effects on Sr partitioning in coccoliths of multiple species of coccolithophorids in culture. Global and Planetary Change (in press).

Stoll, H.M., Schrag, D.P., Clemens, S.C., 1999. Are seawater Sr/Ca variations preserved in Quaternary foraminifera? Geochim. Cosmochim. Acta 63, 3535–3547.

Stoll, H.M., Klaas, C., Probert, I., Ziveri, P., Ruiz-Encinar, J., Garcia-Alonso, J.I., 2000. Sr/Ca of coccolith carbonate: testing the story of the smallest carbonate repositories. Journal of Nannoplankton Research 22, 142.

Thierstein, H.R., Roth, P.H., 1991. Stable isotopic and carbonate cyclicity in Lower Cretaceous deep-sea sediments: dominance of diagenetic effects. Marine Geology 97, 1–34.

Tremolada, F., Erba, E., 2000. Late Valanginian and Early Aptian Nannoconid crisis: a phytoplankton response to large igneous events?. Journal of Nannoplankton Research 22, 147.

Tremolada, F., Locatelli, C., Erba, E., 1999. Calcareous nannofossil fluctuations in the Barremian–Aptian: response of phytoplankton to fertility changes. European Union of Geosciences, 10.

Turekian, K.K., 1963. Rates of calcium carbonate deposition by deep-sea organisms, molluscs, and the coral-algae association. Nature 197, 277–278.

Watkins, D.K., 1989. Nannoplankton productivity flucutations and rhythmically-bedded pelagic carbonates of the Greenhorn Limestone (Upper Cretaceous). Palaeogeog., Palaeoclimat., Palaeoecol. 74, 75–86.

Weissert, H., Lini, A., Follmi, K.B., Kuhn, O., 1998. Correlation of Early Cretaceous carbon isotope stratigraphy and platform drowning events: a possible link? Palaeogeog., Palaeoclimat., Palaeoecol. 137, 189–203.

Young, J.R., 1994. Functions of coccoliths. In: Winter, A., Siesser, W. (Eds.), Coccolithophorids. Cambridge University Press, Cambridge, pp. 63–82.